

THE PROPERTIES OF X-RAY SELECTED ACTIVE GALACTIC NUCLEI. II. A DEEPER LOOK AT THE COSMOLOGICAL EVOLUTION

ROBERTO DELLA CECA,^{1,2} TOMMASO MACCACCARO,^{2,3,4} ISABELLA M. GIOIA,^{5,6,7}
 ANNA WOLTER,^{3,7} AND JOHN T. STOCKE⁸

Received 1991 July 19; accepted 1991 October 29

ABSTRACT

Using a sample of 448 X-ray selected active galactic nuclei extracted from the *Einstein Observatory* Extended Medium Sensitivity Survey we have investigated in greater detail than previously done their cosmological evolution. The data have been analyzed within the framework of pure luminosity evolution (PLE) models and the two most common evolutionary forms $L_x(z) = L_x(0)e^{Cz}$ and $L_x(z) = L_x(0)(1+z)^C$ have been considered. Using a method that allows us to investigate luminosity evolution in redshift or luminosity shells we find evidence for luminosity-dependent luminosity evolution (LDLE) if the evolution function has the exponential form. However, the evidence for luminosity-dependent evolution becomes marginal if the data are fitted with a power-law evolution function and the simpler PLE model is, in this case, still acceptable. Similar results were obtained, in the optical domain, from the analysis of a sample of optically selected QSOs with $z < 2.2$ and $B < 20$. The EMSS AGNs X-ray number-flux relationship has been obtained. It can be described by a power-law $N(>S) = K \times S^{-\alpha}$ with best-fit value for the slope $\alpha = 1.61 \pm 0.06$. It has been compared with the extragalactic *ROSAT* $\log N(>S) - \log(S)$ recently obtained and a good agreement is found.

Subject headings: cosmology: observations — galaxies: evolution — galaxies: nuclei — X-rays: galaxies

1. INTRODUCTION

Active Galactic Nuclei (AGNs),⁹ whether discovered in the optical, radio, or X-ray domain, show definitive marks of a substantial evolution with cosmic time (Schmidt 1968; Maccacaro & Gioia 1983). Deciphering the way in which AGNs evolve is not only a statistical exercise but it also provides an essential constraint on how the population characteristics have changed with time. If the evolution of the ensemble can be satisfactorily described, some clues may be inferred for the evolution of individual sources, and therefore for the physics of the AGNs phenomenon (Cavaliere, Morrison, & Wood, 1971; Cavaliere, Giallongo, & Vagnetti 1985; Caditz & Petrosian 1990; Caditz, Petrosian, & Wandel 1991). The determination of the AGNs cosmological evolution is also important to evaluate their contribution to the X-ray background, to estab-

lish the epoch of their formation and to evaluate their contribution to the heating and ionization of the intergalactic medium. Cosmological evolution may also provide important clues to reveal the connection between AGNs and normal galaxies (e.g., Cavaliere & Padovani 1989).

The major contending models proposed to describe the evolution of quasars are pure density evolution (PDE) (Schmidt 1968) and pure luminosity evolution (PLE) models (Mathez 1976; 1978). More complicated forms have been proposed, such as luminosity-dependent density evolution (Schmidt & Green 1983; 1986), luminosity-dependent luminosity evolution (Cavaliere et al. 1983) or luminosity-density evolution (Koo 1983). If the entire luminosity function (LF) were sampled at all redshifts, then one could easily discriminate between the different models since, for instance, PDE requires the total number of objects to change with time, while PLE requires that the total number remains constant. However, as a consequence of dealing with flux-limited samples, there is a maximum allowed redshift at any given intrinsic luminosity, or a minimum detectable luminosity at any given redshift. In other words, different parts of the luminosity function are sampled at different redshifts. In principle, bright objects may be detected at low redshifts, but due to the small volume sampled and to the slope of the luminosity function, the product volume times luminosity function (i.e., the number of objects) turns out to be so low that none, or very few, high-luminosity objects are seen. This limitation does not depend on the limiting flux, as is the case for high-redshift objects, but on the area of sky covered by the survey.

In Maccacaro et al. (1991; hereafter Paper I), we have performed an analysis of the cosmological evolution of X-ray-selected AGNs using a sample of 448 objects extracted from the *Einstein Observatory* Extended Medium Sensitivity Survey

¹ Dipartimento di Astronomia, Università di Bologna, via Zamboni 33, 40126 Bologna, Italy.

² Osservatorio Astronomico di Bologna, via Zamboni 33, 40126 Bologna, Italy.

³ Osservatorio Astronomico di Brera, via Brera 28, 20121 Milano, Italy.

⁴ Also from Istituto di Fisica Cosmica del Consiglio Nazionale delle Ricerche, via Bassini 15, 20133 Milano, Italy.

⁵ Istituto di Radioastronomia del Consiglio Nazionale delle Ricerche, via Irnerio 46, 40126 Bologna, Italy.

⁶ Visitor at the Institute for Astronomy, University of Hawaii, 2680 Woodlawn Drive, Honolulu, HI 96822.

⁷ On leave of absence from Harvard-Smithsonian Center for Astrophysics, 60 Garden Street, Cambridge, MA 02138.

⁸ Center for Astrophysics and Space Astronomy, University of Colorado, Campus Box 391, Boulder, CO 80309.

⁹ As in previous papers, with the term AGNs we refer to QSOs and Seyfert nuclei, but not to BL Lac objects which show different evolutionary properties (Woltjer & Setti 1982; Maccacaro et al. 1984; Morris et al. 1991).

(EMSS).¹⁰ As we noted in Paper I, we are not yet in the position to unequivocally determine the evolutionary law which best describes the AGN behavior. To do so, a sampling of the luminosity function over a broader range of luminosities at each redshift is needed. Consequently, we have used the V_e/V_a method (Avni & Bahcall 1980) to determine the best-fit parameters of the assumed evolutionary models. Since in the case of quasars PDE models fail to describe the observed counts at faint magnitudes (Braccetti et al. 1980; Koo & Kron 1982) the data were analyzed within the framework of PLE considering the two most common evolutionary forms, $L_x(z) = L_x(0)e^{Cz}$ and $L_x(z) = L_x(0)(1+z)^C$. The much enlarged statistics with respect to the original MSS sample of AGNs (Maccacaro, Gioia, & Stocke 1984) allowed us to derive tighter limits on the confidence intervals for the evolution parameter C .

In this paper we will consider in more detail the two models already analyzed in Paper I in order to establish which is the most appropriate representation of the evolution for X-ray selected AGNs and whether there is any evidence for luminosity dependent evolution. We will use the same 448 AGNs as in Paper I. In § 2 we describe the procedure utilized to study the cosmological evolution within redshift and/or luminosity shells. In § 3 we will apply the procedure to the data and discuss the results obtained. In § 4 the AGNs $\log N - \log S$ is derived and compared with the recently determined extragalactic ROSAT $\log N - \log S$ for 39 sources detected in a 0.35 deg² deep survey area (Shanks et al. 1991). In § 5 a summary and conclusions are presented.

Throughout the paper a Hubble constant of 50 km s⁻¹ Mpc⁻¹ and a Friedmann universe with a deceleration parameter $q_0 = 0$ are assumed. All the data used in this paper are published in Paper I. Thus the reader interested in computing one or more quantities under different assumptions can do so.

2. PROCEDURE

The V_e/V_a variable (Avni & Bahcall 1980), a generalization of the V/V_{\max} method (Schmidt 1968) when several complete samples of objects are combined, is a powerful tool to study the cosmological evolution of a class of objects. The test statistic is the ratio of the volume enclosed by the redshift of the object (V_e) over the maximum volume, the volume available (V_a), within which a given object can be seen and still be part of the sample. The test can be used to check the completeness of the sample as well as to evaluate, in the case of statistically complete samples, the cosmological evolution of the objects. In the case of a statistically complete sample of objects which are uniformly distributed, the above test yields a mean $\langle V_e/V_a \rangle = 0.50$ and a uniform distribution of the individual values of V_e/V_a between 0 and 1.

We have found in Paper I that the hypothesis of a uniform distribution for the EMSS AGNs is rejected at high signifi-

cance ($\langle V_e/V_a \rangle = 0.6194 \pm 0.0136$). Thus the data set was analyzed within the framework of PLE considering the two most common evolutionary forms, the exponential evolution model (eq. [1]) and the power law evolution model (eq. [2]):

$$L_x(z) = L_x(0)e^{Cz}, \quad (1)$$

$$L_x(z) = L_x(0)(1+z)^C, \quad (2)$$

where $L_x(0)$ is the present epoch ($z = 0$) luminosity, C is the evolution parameter and $\tau = z/(1+z)$ is the look-back time.

To analyze the cosmological properties of a subsample of objects, defined by the luminosity interval ΔL and the redshift interval Δz in the L_x-z plane, we must take into proper account all the bounds imposed by the definition criteria of the subsample. Let us consider in the L_x-z plane an object approaching z_{\max} . This object is still part of a given subsample until its flux remains larger than (or equal to) the survey flux limit. Since in the framework of luminosity evolution, the luminosity of an object evolves according to the assumed model, an object approaching z_{\max} can exit from the subsample defined for instance by the luminosity interval ΔL . The bounds imposed by the redshift shell into consideration must also be taken into account.

These effects are illustrated in Figure 1 for four typical cases. The filled squares (labeled as A, B, C, D) represent four objects in the subsample defined by $\Delta L_x, \Delta z$. The solid lines represent how the objects move in the L_x-z plane according to the assumed evolutionary model, while the dot-dashed line represents the limiting flux of the survey for which a solid angle Ω_i has been covered. The box described by the dashed lines indicates the boundaries of the considered sample ($42.9 < \Delta \log L_x < 45; 0.04 < z < 0.3$).

As can be seen, object A is bound by the lower limit of the luminosity shell and by the limiting flux of the survey; object B is bound by the lower limit of the redshift shell and by the limiting flux of the survey; object C is limited only by the lower and upper limits of the redshift shell into consideration; object D is limited by the lower bound of the redshift shell and by the upper bound of the luminosity shell into consideration.

To analyze the cosmological evolution of subsamples defined by redshift and/or luminosity shells all these bounds must be taken into account when computing the values of V_e and V_a . The procedure to use is thus as follows. For each AGN (inside $\Delta L_x \times \Delta z$) characterized by its redshift z_{obj} and its observed luminosity L_x , and for the assumed evolutionary model $f(z)$, we have computed the "de-evolved" zero redshift luminosity $L_x(0)$. The values of V_a and V_e have been computed in the following manner:

$$V_a = \sum_{i=1,j} \frac{\Omega_i}{4\pi} [V(z_{\max i}) - V(z_{\min i})],$$

$$V_e = \sum_{i=1,j} \frac{\Omega_i}{4\pi} \{V[\min(z_{\text{obj}}, z_{\max i})] - V(z_{\min i})\},$$

where (a) the sum is carried out over the different flux limits f_{lim_i} of the survey; (b) Ω_i is the solid angle of the sky searched at f_{lim_i} ; (c) $z_{\max i}$ is the *minimum* between: (1) the upper bound of the redshift shell under consideration; (2) the maximum z at which the source can be detected with a flux greater or equal than f_{lim_i} ; (3) the maximum z imposed by the condition that the object luminosity, $L_x(z) = L_x(0) \times f(z)$, falls within the

¹⁰ For a full description of the EMSS, the selection criteria and data analysis, the reader is referred to Gioia et al. (1990) where the sample of sources is given. A detailed discussion of the identification process and of the optical properties of the EMSS X-ray sources is given in Stocke et al. (1991). The optical images of the area surrounding the EMSS sources will be shown in Maccacaro et al. (1992). Here we recall that the EMSS is a statistically complete and well-defined sample of 835 serendipitous X-ray sources detected in the images of the high galactic latitude sky obtained with the Imaging Proportional Counter on board the *Einstein Observatory*. The EMSS has limiting sensitivities in the range 5×10^{-14} – 3×10^{-12} ergs cm⁻² s⁻¹ (0.3–3.5 keV). The sky coverage for the survey, computed assuming a power-law spectrum with energy index $\alpha = 1$, is reported in Table 2 of Paper I.

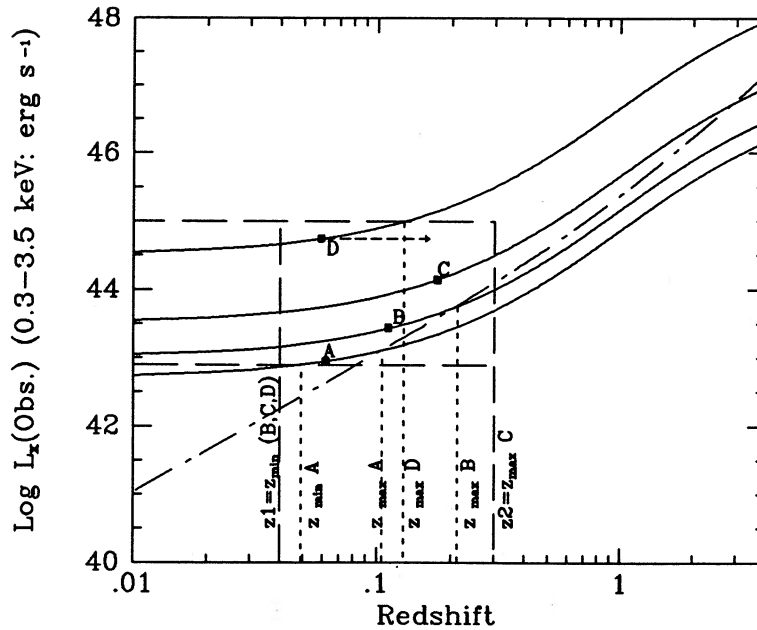


FIG. 1.—A sketch of the L_x - z plane showing the effects described in the text (see § 2). The filled squares (labeled as A, B, C, D) represent four hypothetical objects of the sample. The solid lines represent how the objects move in the L_x - z plane according to the assumed PLE model, while the dot-dashed line represents the survey flux limit. The box described by the dashed lines indicates the boundaries of the considered sample. The arrow shows how the object D moves in the case of density evolution or no evolution.

required luminosity bin; (d) z_{\min} is the *maximum* between: (1) the lower bound of the redshift shell under consideration and (2) the minimum z imposed by the condition that the object luminosity $L_x(z) = L_x(0) \times f(z)$ falls within the required luminosity bin.

We have then assumed the evolutionary laws of equation (1) or equation (2), and we have searched which values of the evolution parameter C yield $\langle V_e/V_a \rangle = 0.5$ and a uniform distribution (between 0 and 1) of the individual V_e/V_a values. The 1σ interval on C corresponds to the values for which $\langle V_e/V_a \rangle = 0.5 \pm 1/(12N)^{1/2}$, where N is the number of objects in the sample.

Using the above procedure is thus possible to analyze the cosmological evolution within selected regions $\Delta L \times \Delta z$ of the L_x - z plane. However, to do so, one still needs a larger number of objects and a more uniform coverage of the L_x - z plane than presently at our disposal. Therefore we shall limit our analysis to redshift bins *or* luminosity bins. Considering the AGNs within redshift shells, regardless of their luminosity, it is possible to study the cosmological evolution in redshift intervals. On the other hand, if we consider the AGNs with *observed* luminosity in a defined luminosity interval, regardless of their redshift, we can study the cosmological evolution as a function of luminosity.

To test the correctness of this procedure we have applied it to a set of simulated samples described by the PLE forms given in equation (1) or equation (2). The evolution parameter C has been set to 4.18, for the exponential evolution model, and to 2.56, for the power-law evolution model (i.e., the best-fit values of the EMSS AGNs sample found in Paper I). The simulated samples have been generated using the EMSS sky coverage but with a number of objects over than twice the number of the real sample so as to reduce the statistical uncertainties. Each simulated sample has been analyzed within the same evolutionary model used to generate it.

In the case of luminosity evolution analysis in luminosity

bins, we have considered four intervals: $\Delta L_1 = [10^{42} - 10^{43.5}]$; $\Delta L_2 = [10^{43.5} - 10^{44.25}]$; $\Delta L_3 = [10^{44.25} - 10^{45}]$; $\Delta L_4 = [10^{45} - 10^{48}]$ ergs s^{-1} . The results of the analysis are shown in Figure 2a (exponential evolution model) and Figure 2b (power-law evolution model). The 68% confidence intervals on the evolution parameters C are shown (*vertical solid line*). The horizontal dashed lines indicate the 68% confidence intervals for C obtained using the whole sample of objects. As expected the values of C obtained for different ΔL are consistent with each other and with the value resulting from the analysis of the whole sample. Consistent results have been obtained using the other simulated samples as well as performing the luminosity evolution analysis in redshift bins. This gives us confidence that the procedure is correct. We note that the 68% confidence interval for the weakest objects (ΔL_1) is so large that C is basically undetermined. It has to be appreciated that, because we used the EMSS sky coverage to simulate the samples, the lowest luminosity interval contains only low-redshift objects. In this domain the V_e/V_a method is rather insensitive to different evolution models and/or different values of the evolution parameter. Nothing can be said on the cosmological evolution of these low-luminosity objects. As already noted by Marshall (1985), $\langle V_e/V_a \rangle = 0.5$ for these objects *does not* necessarily rule out strong evolution.

The procedure described above is general and can be applied also when examining density evolution models or models with no evolution. In both cases objects move, in the L_x - z plane, parallel to the redshift axis (see arrow on object D in Fig. 1) and thus the luminosity bin ΔL into consideration does not play any role on the redshift limits. In the next section we will apply this procedure to the EMSS sample of AGNs to study their cosmological evolution in both redshift and luminosity bins.

3. LUMINOSITY-DEPENDENT LUMINOSITY EVOLUTION

If a population of objects evolves according to a PLE model and if we are considering the “true” evolution law, then the

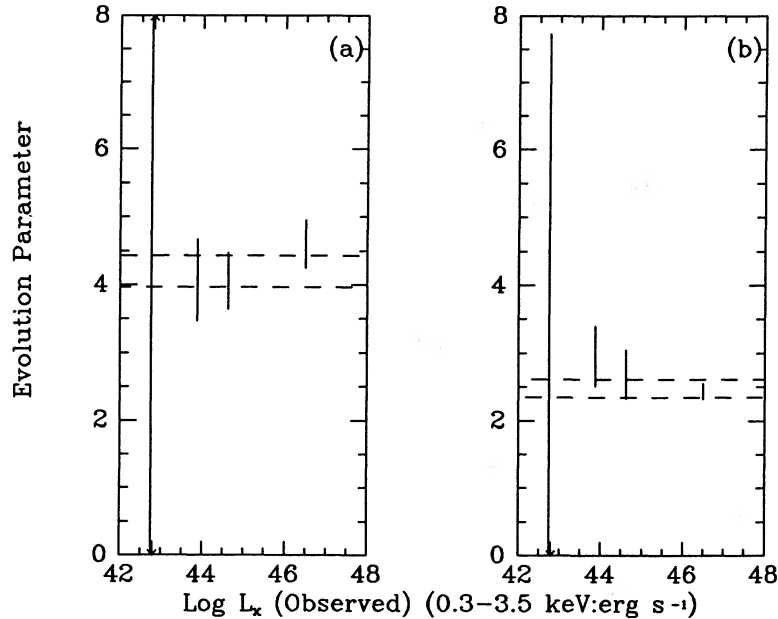


FIG. 2.—Results of the luminosity evolution analysis in luminosity bins ΔL [$\Delta L_1 = [10^{42}-10^{43.5}]$; $\Delta L_2 = [10^{43.5}-10^{44.25}]$; $\Delta L_3 = [10^{44.25}-10^{45}]$; $\Delta L_4 = [10^{45}-10^{48}]$ ergs s^{-1}] for the simulated samples. Each simulated sample has been analyzed within the same evolutionary model used to create it. The 68% confidence intervals on the evolution parameters C are shown (vertical solid lines). Dashed lines indicate the 68% confidence intervals for C obtained using the whole sample of objects. (a) PLE model of exponential form; (b) PLE model of power-law form. See § 2 for details.

evolution of low- and high-redshift objects should be successfully described by the same parameter(s). To see if this is the case for our sample of X-ray selected AGNs we have first pursued the analysis of the cosmological evolution within two redshift bins.

3.1. Redshift Bins

In order to divide the sample into two similarly populated subsamples we have chosen a dividing value of $z = 0.3$. There are 246 objects with redshift less than 0.3 and 202 objects with

redshift greater than 0.3. We have then applied the procedure described in the previous section to the two EMSS AGNs subsamples. The results obtained from the evolution analysis are shown in Figure 3a (exponential evolution model) and Figure 3b (power-law evolution model). Best-fit values for C and the associated 68% confidence intervals are shown. The horizontal solid line indicates the best-fit value obtained using the total sample, while the two dashed lines indicate the corresponding 68% confidence interval for C (see Paper I). For the exponential evolution model, there is evidence that AGNs with

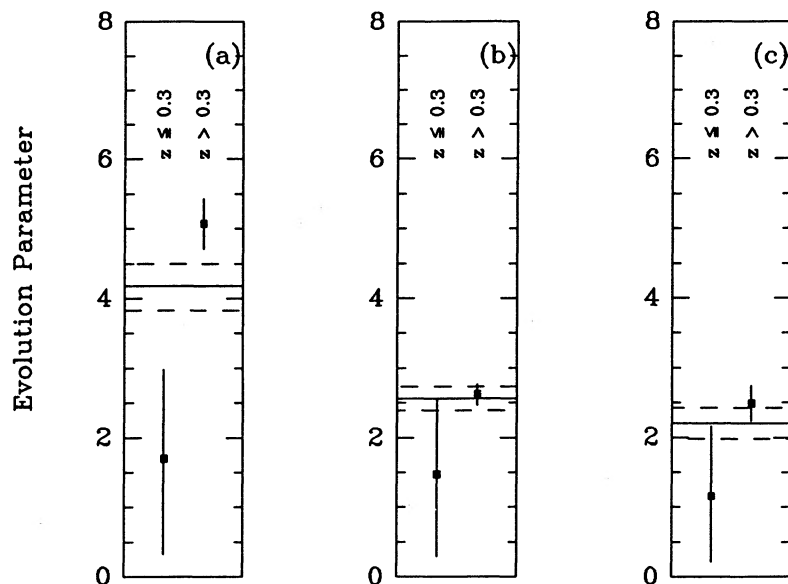


FIG. 3.—Results of the evolution analysis of the EMSS AGNs obtained dividing the sample into two redshift bins ($z \leq 0.3$ and $z > 0.3$). The best fit values for C and the associated 68% confidence intervals are shown. The horizontal solid line indicates the best-fit value obtained using the total sample, while the two dashed lines indicate the corresponding 68% confidence interval for C . (a) PLE model of exponential form; (b) PLE model of power-law form; (c) luminosity-dependent luminosity evolution model of exponential form as given in eq. (3). See § 3 for details.

$z > 0.3$ cannot be fitted by the same evolution parameter as those with $z < 0.3$. The best-fit values are $C = 1.70$ ($\pm 1 \sigma = 0.33$ – 2.98) for $z < 0.3$ and $C = 5.08$ ($\pm 1 \sigma = 4.71$ – 5.43) for $z > 0.3$, whereas the entire data set is fitted by $C = 4.18$ ($\pm 1 \sigma = 3.83$ – 4.50). The difference between the evolution parameter values in the two redshift bins is significant at the 3σ level. The exponential PLE model is not an appropriate representation of the data since it fails to describe simultaneously the cosmological properties of both low- and high-redshifts objects. Thus we can rule out a PLE evolution with exponential form, as given by equation (1).

Using the power-law model, instead, one finds $C = 1.47$ ($\pm 1 \sigma = 0.29$ – 2.56) and $C = 2.63$ ($\pm 1 \sigma = 2.47$ – 2.77) for the low- and high-redshift samples, respectively, whereas the entire data set is fitted with $C = 2.56$ ($\pm 1 \sigma = 2.39$ – 2.73). These values are consistent within the errors.

As a consequence of dealing with flux-limited samples, redshift and luminosities are heavily coupled ($\langle \log L_x \rangle = 43.7$ and 45.0 for the low- and the high-redshift bin, respectively). The difference we have found with the exponential PLE model could be due to the difference in the luminosity distribution of the two subsamples. In other words, if AGNs are characterized by luminosity dependent evolution, the division of the sample into low- and high-redshift subsamples results in a division in low- and high-luminosity objects. Therefore, one should expect to see a difference in the evolutionary properties of high- and low-redshift subsamples due to the different luminosity distribution. Thus, it is interesting to analyze the cosmological evolution in luminosity bins in order to establish if there is any evidence of luminosity-dependent luminosity evolution.

We note here that the choice of $z = 0.3$ allows us to make an appropriate comparison between our results and those obtained by investigators working at optical wavelengths. Optical samples, in fact, are usually incomplete at low redshift (among other reasons QSOs appear “extended” on photographic plates). To properly consider this incompleteness, evolu-

tionary analyses in the optical domain are carried out for values of z greater than ~ 0.3 (e.g., see Boyle et al. 1990) or for luminosities greater than some critical luminosity (e.g., Marshall 1985; $M_B < -23$). Recently Boyle et al. (1990) investigated the cosmological evolution of optically selected quasars by analyzing a sample of ~ 600 objects. Within the framework of the two luminosity evolution laws considered in this paper and restricting the analysis only to objects with $M_B < -23$ and $z > 0.3$, they found best-fit values of 7.0 ± 0.10 for the PLE model in the exponential form and 3.46 ± 0.10 for the same model in the power-law form. Their results can be compared with the results we have obtained for our high-redshift sample. In fact, this sample contains, by definition, objects with z greater than 0.3 and only $\sim 10\%$ of them have M_B greater than -23 . Despite the larger best-fit value of the evolution parameter(s) for the high-redshift subsample ($C_{z>0.3} = 5.08$ and 2.63 for the exponential and power-law evolution model, respectively) relative to the entire data set ($C = 4.18$ and 2.56) the “slower” X-ray evolution, first noted by Maccacaro & Gioia (1983), is confirmed.

3.2. Luminosity Bins

We have divided the sample of EMSS AGNs in the same luminosity bins as the simulated samples in § 2. In each luminosity bin there are, respectively, 82, 154, 132, and 80 AGNs.

The results of the analysis are shown in Figure 4a (exponential evolution model) and Figure 4b (power-law evolution model). The best-fit values and the 68% confidence intervals for the evolution parameters C are shown (vertical solid line). The dashed lines indicate the 68% confidence intervals for the evolution parameters C obtained using the whole sample of EMSS AGNs (see Paper I). In the case of the exponential evolution model (Fig. 4a) there is evidence for luminosity-dependent luminosity evolution as it is expected from the analysis of low- versus high-redshift objects. The value of the evolution parameter C depends on the luminosity

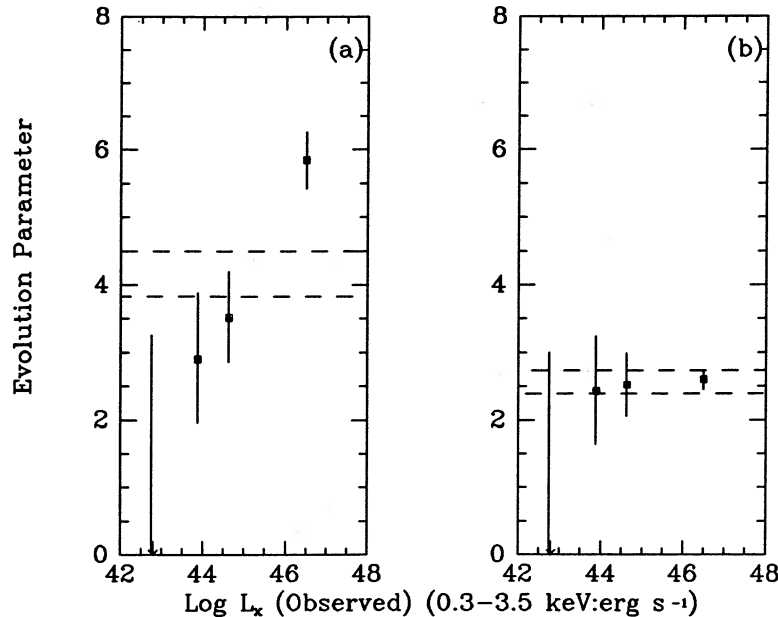


FIG. 4.—Results on the luminosity evolution analysis in luminosity bins ΔL for the EMSS AGNs sample. The luminosity bins are the same as the simulated ones. The best-fit values for C (luminosity bins: ΔL_2 , ΔL_3 , and ΔL_4) and the associated 68% confidence intervals are shown. The dashed lines indicate the 68% confidence intervals for C obtained using the whole sample of objects. (a) PLE model of exponential form; (b) PLE model of power-law form. See § 3 for details.

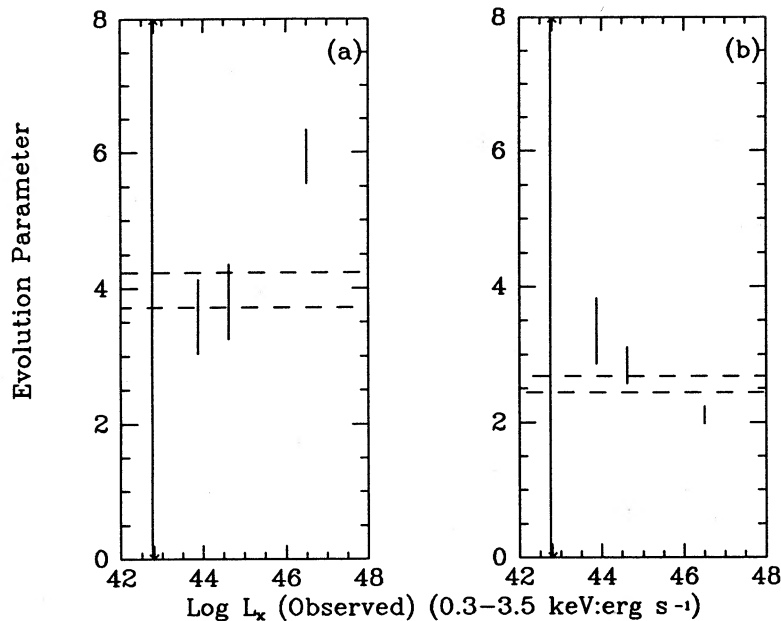


FIG. 5.—Results on the luminosity evolution analysis in luminosity bins ΔL on the simulated samples. Each simulated sample has been analyzed with an evolutionary model different from that used to generate it. The 68% confidence intervals on the evolution parameters C are shown (vertical solid line). The dashed lines indicate the 68% confidence intervals for C obtained using the whole sample of objects. (a) Sample simulated with the PLE model of power-law form and analyzed with the PLE model of exponential form; (b) sample simulated with the PLE model of exponential form and analyzed with the PLE model of power-law form. See § 3 for details.

and the best-fit intervals for ΔL_2 ($C = 2.90$; $\pm 1 \sigma = 1.96$ – 3.88) and ΔL_4 ($C = 5.85$; $\pm 1 \sigma = 5.42$ – 6.26) are different at the 2.90σ level.¹¹ However, luminosity-dependent luminosity evolution is not required if the evolution function is given by a power law.¹²

We have been prompted by these results to consider again the simulated samples to examine what happens when a sample constructed with a particular evolution model is analyzed with a different model.

The results of the analysis are given in Figure 5a (sample simulated with the power-law evolution model and analyzed with the exponential evolution model) and Fig. 5b (sample simulated with the exponential evolution model and analyzed with the power-law evolution model). As in previous figures the 68% confidence intervals on the evolution parameters C are shown (vertical solid line) as well as the 68% confidence intervals for the evolution parameters C obtained using the whole sample of objects (horizontal dashed lines). In Figure 5a we see that the sample simulated with the power-law evolution model shows a luminosity-dependent luminosity evolution if it is analyzed with the exponential model. The values for the evolution parameter C for the luminosity bins ΔL_2 and ΔL_4 are significantly different. A similar effect is visible in Figure 5b where the sample simulated with the exponential evolution model is analyzed with the power-law evolution model.

Similar results were obtained, in the optical domain, by Marshall (1985) from the analysis of a sample of optically selected QSOs with $z < 2.2$ and $B < 20$. The method used by

Marshall (1985) assumes pure density evolution in order to investigate “local” phenomena (small regions of the L_x - z plane). Marshall (1985) found that luminosity-dependent density evolution is needed if the evolution function has an exponential form, while no luminosity-dependent density evolution is required if the data are analyzed with a power-law density evolution model. His conclusions hold also for luminosity evolution models provided that the luminosity function is described by a featureless power law whose slope does not vary with redshift. Our method has the advantage of requiring no assumptions on the form of the luminosity function. We analyzed directly luminosity evolution in luminosity intervals. The present data set, however, does not take full advantage of the method utilized. The AGNs in the EMSS that give any leverage of the evolution are the ones with $L_x > 10^{43.5}$ ergs s^{-1} and the XLF in this range is adequately characterized by a single power law (see Figs. 6 and 9 in Paper I). Therefore the application of Marshall (1985) method is equally appropriate. Our method should be more appropriate to analyze deeper X-ray surveys which will sample low-luminosity ($\log L_x < 43.5$) high-redshifts objects (e.g., *ROSAT* deep surveys).

To summarize, our analysis indicates that the evolution of X-ray selected AGNs can be described either by a PLE model of the power-law form (eq. [2]) or by a LDLE¹³ model of exponential form.

¹³ A different kind of luminosity dependent evolution—luminosity-dependent density evolution—has been proposed by Schmidt & Green (1983) to explain the evolutionary properties of the “bright” quasar sample. Their proposed dependence, adapted to the case of X-ray luminosity, becomes

$$\rho(z, L_x) = e^{k_D \rho (\log(L_x) - 42)z}, \quad (4)$$

where $\rho(z, L_x)$ is the density evolution law, L_x is the observed luminosity, and k_D is the density evolution parameter. We find that our data set is best described by $k_D = 2.97$ with associated 68% and 95% confidence intervals of (2.64–3.31) and (2.30–3.66), respectively. The evolution law of equation (4) is accepted by the KS test at the 95% confidence level.

¹¹ The choice of ΔL_2 instead of ΔL_1 , to compare with ΔL_4 is due to the fact that, as discussed previously, the evolution parameter is only very poorly determined in ΔL_1 .

¹² We have also investigated the effect of the assumption that the X-ray spectrum is described by a power-law energy index $\alpha_E = 1$ on the determination of the cosmological evolution. Since $\alpha_E \neq 1$ leads to the introduction of a K -correction of the form $(1+z)^{1-\alpha_E}$ the net effect is, in first approximation, that one obtains a best-fit value for C (PLE model of power-law form) which is higher (if $\alpha_E > 1$) or lower (if $\alpha_E < 1$) by an amount $d \approx |1 - \alpha_E|$ (for $d < 1$).

To quantify this luminosity dependence we have assumed a linear relationship of the evolution parameter k_L on the X-ray luminosity, as given by

$$L_x(z) = L_x(0)e^{k_L(\log [L_x(0)] - 42)\tau} \quad (3)$$

to hold over the range of sampled luminosities. We find that our data set is best described by $k_L = 2.2$ with an associated 68% and 95% confidence intervals of (1.98–2.42) and (1.75–2.64), respectively. The evolution law of equation (3) is accepted by the KS test at the 95% confidence level. This model leads to consistent values of the evolution parameter k_L when low- and high-redshift objects are considered separately (see Fig. 3c). This model also naturally explains the more rapid evolution seen in optically selected sample since X-ray selection favors the discovery of lower luminosity objects due to the observed $L_x \propto L_{\text{opt}}^{(0.7-0.8)}$ dependence (Avni & Tananbaum 1986).

At present we cannot distinguish between the two evolutionary forms given by equation (2) and equation (3). Most of the EMSS AGNs are characterized by an X-ray luminosity around $\sim 10^{44}$ ergs s^{-1} and have redshifts of 2 or less. At these luminosities and redshifts the two evolution models lead to very similar brightening factors. On the contrary they diverge either for low-luminosity ($\sim 10^{42-43}$ ergs s^{-1})—high-redshift ($z > 1$) sources or for high-luminosity ($\gtrsim 10^{46}$ ergs s^{-1}) sources. The former are unfortunately unobservable at present, since they have an X-ray flux less than 10^{-15} ergs cm^{-2} s^{-1} and the latter are relatively rare objects. However, a survey of the whole sky with a limit sensitivity of 10^{-12} ergs cm^{-2} s^{-1} or slightly better (e.g., the *ROSAT* All Sky Survey) should be able to detect enough of these latter sources to allow discriminating between the two models. Nevertheless, it is worth noting that, as simple models have increasing difficulty in explaining the available data, models with a more specific physical basis, like LDLE (Cavaliere et al. 1983), begin to be necessary to describe the cosmological evolution of AGNs.

4. THE COMPARISON BETWEEN THE EMSS AND *ROSAT* $\log(N) - \log(S)$'s

The much larger EMSS sample, with respect to the original MSS sample (Gioia et al. 1984), and the very high identification rate presently available (96%) allow us to update the determination of the number-flux relationship for the class of X-ray selected AGNs. The EMSS AGNs $\log N(>S) - \log S$, presented here for the first time, is shown in Figure 6. It can be described by a power law $N(>S) = K \times S^{-\alpha}$ with best-fit value for the slope $\alpha = 1.61 \pm 0.06$ and $K = 4.92 \times 10^{-21}$ deg $^{-2}$. It has been truncated at 1×10^{-11} ergs cm^{-2} s^{-1} since the EMSS may not be complete at such a high flux level (see Gioia et al. 1990 for details). The parameters are derived applying the maximum likelihood method to the unbinned data (see Gioia et al. 1984 for details on the method). The best fit slope of the EMSS AGNs $\log N(>S) - \log S$ agrees, within the errors, with the $\log N(>S) - \log S$ previously determined using the AGNs in the MSS sample (Gioia et al. 1984).

New data are now becoming available through the *ROSAT* mission. The *ROSAT* PSPC in pointed mode has a lower instrumental background and better spatial resolution which lead to greater sensitivity than the *Einstein* IPC. Sources at fainter fluxes can be seen in long exposure times. Thus, it is interesting to compare these new data with our $\log N(>S) - \log S$.

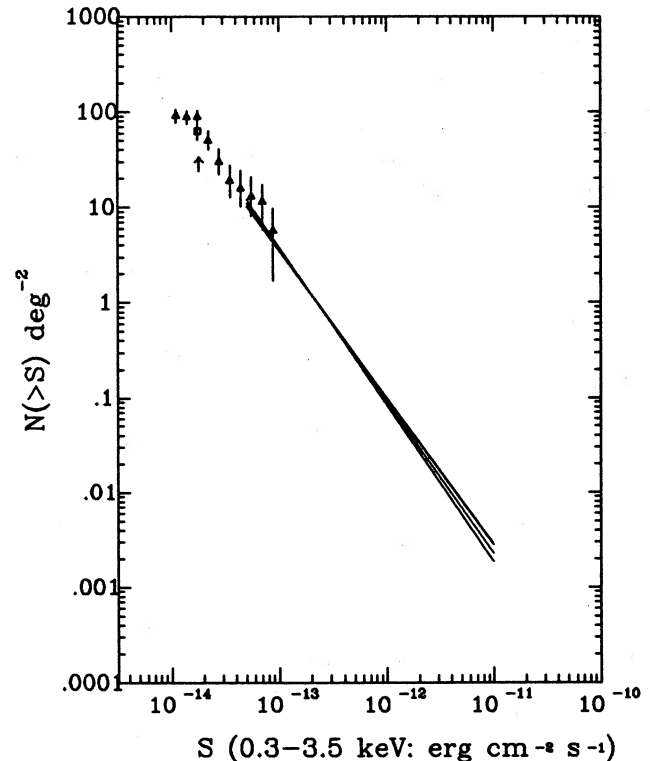


FIG. 6.—The solid lines represent the EMSS AGNs $\log N(>S) - \log S$ (best-fit and $\pm 1 \sigma$ errors on the slope). The filled triangles represent the nonstellar *ROSAT* $\log N(>S) - \log S$ relationship converted from the (0.5–2.0) keV into the (0.3–3.5) keV energy band. The open square represents the *ROSAT* QSOs space density at the completeness limit (arrow) of the Shanks et al. (1991) survey. One sigma error bars are determined by the number of objects which contribute to each bin. See § 4 for details.

Eight *ROSAT* PSPC observations, with exposure time greater than 8000 s, have been searched for discrete sources (*ROSAT* Medium Sensitivity Survey; Hasinger, Schmidt, & Trümper 1991). In the total area surveyed (~ 2.6 deg 2), 184 sources with X-ray flux between 10^{-14} and 2×10^{-13} ergs cm^{-2} s^{-1} (0.1–2.4 keV energy band) have been detected. Furthermore one deep PSPC exposure ($\sim 30,000$ s) has been obtained and analyzed by Shanks et al. (1991). Thirty-nine sources with flux in the range 8.8×10^{-15} – 6×10^{-13} ergs cm^{-2} s^{-1} (0.1–2.4 keV energy band) were detected in 0.35 deg 2 of sky. Above their quoted completeness limit of $\sim 2 \times 10^{-14}$ ergs cm^{-2} s^{-1} (0.1–2.4 keV energy band) 32 sources are found. While the *ROSAT* Medium Sensitivity Survey of Hasinger et al. (1991) has not been spectroscopically identified, the Shanks et al. (1991) survey has a fairly high identification rate ($\sim 77\%$). We will make use of the Shanks et al. (1991) data set to compare the extragalactic *ROSAT* $\log N(>S) - \log S$ (reported in Fig. 4 of Shanks et al. 1991) with the EMSS $\log N(>S) - \log S$.

To this end we need to convert the fluxes from the (0.5–2.0) keV into the (0.3–3.5) keV energy band. We assume a power-law spectrum with energy index $\alpha = 1$ (derived in the spectral analysis of the extragalactic EMSS sources of Maccacaro et al. 1988), the same spectral index used to convert both the *ROSAT* PSPC counts and the *Einstein* IPC counts into fluxes in their respective energy bands. Fluxes are corrected for galactic absorption. The resulting conversion factor from the (0.5–2.0) keV to the (0.3–3.5) keV band is 1.772. The extragalactic

ROSAT $\log N(>S)$ – $\log S$ (in the 0.3–3.5 keV band) is shown in Figure 6 (filled triangles); also shown are the Shanks et al. (1991) survey completeness limit (arrow) and the reported QSOs space density ($63 \pm 13 \text{ deg}^{-2}$)¹⁴ at this limit (open square). As can be seen there is a good agreement, in the region of overlap, between the *ROSAT* extragalactic $\log N(>S)$ – $\log S$ and the EMSS $\log N(>S)$ – $\log S$, especially if one considers that the conversion between the two bands is made under the simplifying hypothesis of a single power-law spectrum of $\alpha = 1$. The extragalactic $\log N(>S)$ – $\log S$ by Shanks et al. (1991) has a best-fit slope of 1.6 ± 0.3 , to be compared with our determination of 1.61 ± 0.06 . Thus the EMSS slope holds to fluxes of the order of $\sim 2 \times 10^{-14} \text{ ergs cm}^{-2} \text{ s}^{-1}$, strongly suggesting that the AGNs could be still the dominant source population at such low fluxes.

We have tried to impose further constraints on the AGNs cosmological evolution using the two cosmological models that are consistent with the EMSS data. However, for fluxes greater than the Shanks et al. (1991) survey completeness limit the two evolutionary models lead to similar predictions. Nothing can be said on the model which best describes the AGNs evolution until deeper surveys are available (e.g., Windhorst et al. 1992).

We have also reestimated the contribution of the AGNs to the XRB. Within the two cosmological evolution models of equation (2) and equation (3) and taking a $z_{\text{max}} \sim 3$, we find that AGNs contribute $\sim 40\%$ to the 2 keV XRB in either model. This is in agreement with the estimate already reported in Paper I.

5. SUMMARY AND CONCLUSIONS

We have investigated the cosmological properties of X-ray selected AGNs in more detail than previously done. The sample utilized consists of 448 objects extracted from the *Einstein Observatory* Extended Medium Sensitivity Survey, and it is the same sample used in Paper I.

The data have been analyzed within the framework of a pure luminosity evolution model and the two most popular evolutionary forms, $L_x(z) = L_x(0)e^{Cz}$ and $L_x(z) = L_x(0)(1+z)^C$, have been considered.

¹⁴ In the Shanks et al. (1991) sample there are five sources still unidentified above the completeness limit, which have hardness ratio values similar to those found for QSOs (Shanks et al. 1991). If these sources turn out to be QSOs, then the QSOs space density increases to $77 \pm 15 \text{ deg}^{-2}$, to be compared with the extragalactic *ROSAT* space density of $89 \pm 16 \text{ deg}^{-2}$.

In order to establish if there is any evidence of luminosity dependent luminosity evolution we have used the V_o/V_a method to analyze cosmological evolution within redshift and/or luminosity bins. Luminosity-dependent luminosity evolution is necessary if the evolution function has the exponential form. On the contrary, PLE is still acceptable in the case of the power-law evolution form ($C_{\text{bestfit}} = 2.56$).

To quantify this luminosity dependence (in the case of the exponential form), our data have been analyzed within the framework of a luminosity-dependent luminosity evolution model given by $L_x(z) = L_x(0)e^{k_L(\log[L_x(0)]-4.2)z}$. A best-fit value for k_L of 2.2 has been found.

In other words, within the region of the L_x – z plane we sample (L_x from $\sim 10^{42}$ to $\sim 10^{47} \text{ ergs s}^{-1}$ and redshift from 0 to ~ 2) our data are consistent either with a LDLE evolution model with exponential form (like eq. [3]) or with a PLE model with power-law form (eq. [2]). Each of these models leads to identical behavior in the region sampled. Clearly, as one starts sampling higher redshift and lower luminosity regions, the extrapolation of these two models will allow discriminating between them.

The high identification rate (96%) presently available for the *Einstein* Extended Medium Sensitivity Survey allowed us to obtain the $\log N(>S)$ – $\log S$ relation for the class of the X-ray selected AGNs. A best-fit value of $\alpha = 1.61 \pm 0.06$ has been found with an associated normalization $K = 4.92 \times 10^{-21} \text{ deg}^{-2}$ for a power-law description of the number-count relation. This $\log N(>S)$ – $\log S$ has been compared with the recently obtained extragalactic *ROSAT* $\log N(>S)$ – $\log S$. A good agreement is found between the two $\log N(>S)$ – $\log S$, suggesting that the AGNs could be the dominant population at such low fluxes.

Deeper *ROSAT* surveys are needed to impose further constraints on the AGNs cosmological evolution.

We would like to thank G. G. C. Palumbo, G. Setti, and G. Zamorani for useful discussions. Part of the data analysis has been done using the Distributed Information Retrieval from Astronomical Files (DIRA) developed by the Astronet Working Group on Database and Documentation. This work has received partial financial support from NASA contracts NAS 5-1224, NAG 5-1584 and from the Italian Space Agency (ASI). R. D. C. thanks CASA for the warm hospitality during a 2 month visit when part of this work was completed.

REFERENCES

- Avni, Y., & Bahcall, J. N. 1980, *ApJ*, 235, 694
 Avni, Y., & Tananbaum, H. 1986, *ApJ*, 305, 83
 Braccetti, A., Zitelli, V., Bonoli, F., & Formiggini, L. 1980, *A&A*, 85, 80
 Boyle, B. J., Fong, R., Shanks, T., & Peterson, B. A. 1990, *MNRAS*, 243, 1
 Caditz, D., & Petrosian, V. 1990, *ApJ*, 357, 326
 Caditz, D. M., Petrosian, V., & Wandel, A. 1991, *ApJ*, 372, L63
 Cavaliere, A., Giallongo, E., Messina, A., & Vagnetti, F. 1983, *ApJ*, 269, 57
 Cavaliere, A., Giallongo, E., & Vagnetti, F. 1985, *ApJ*, 296, 402
 Cavaliere, A., Morrison, P., & Wood, K. 1971, *ApJ*, 170, 223
 Cavaliere, A., & Padovani, P. 1989, *ApJ*, 340, L5
 Gioia, I. M., Maccacaro, T., Schild, R. E., Stocke, J. T., Liebert, J. W., Danziger, I. J., Kunth, D., & Lub, J. 1984, *ApJ*, 283, 495
 Gioia, I. M., Maccacaro, T., Schild, R. E., Wolter, A., Stocke, J. T., Morris, S. L., & Henry, J. P. 1990, *ApJSS*, 72, 567
 Hasinger, G., Schmidt, M., & Trümper, J. 1991, *A&A*, 246, L2
 Koo, D. C. 1983, in *Proc 24th Liège International Astrophysical Colloquium, Quasars and Gravitational Lenses* (Liège: Université de Liège), 240
 Koo, D. C., & Kron, R. G. 1982, *A&A*, 105, 107
 Maccacaro, T., & Gioia, I. M. 1983, in *Early Evolution of the Universe and its Present Structure*, ed. G. O. Abell & G. Chincharini (Dordrecht: Reidel), 7
 Maccacaro, T., Gioia, I. M., Maccagni, D., & Stocke, J. 1984a, *ApJ*, 284, L23
 Maccacaro, T., Gioia, I. M., & Stocke, J. T. 1984b, *ApJ*, 283, 486
 Maccacaro, T., Gioia, I. M., Wolter, A., Zamorani, G., & Stocke, J. T. 1988, *ApJ*, 326, 680
 Maccacaro, T., Della Ceca, R., Gioia, I. M., Morris, S. L., Stocke, J. T., & Wolter, A. 1991, *ApJ*, 374, 117 (Paper I)
 Maccacaro, T., et al. 1992, in preparation
 Marshall, H. L. 1985, *ApJ*, 299, 109
 Mathez, G. 1976, *A&A*, 53, 15
 ———. 1978, *A&A*, 68, 71
 Morris, S. L., Stocke, J. T., Gioia, I. M., Schild, R. E., Wolter, A., Maccacaro, T., & Della Ceca, R. 1991, *ApJ*, 380, 49
 Schmidt, M. 1968, *ApJ*, 151, 393
 Schmidt, M., & Green, R. F. 1983, *ApJ*, 269, 352
 ———. 1986, *ApJ*, 305, 68
 Shanks, T., Georgantopoulos, I., Stewart, G. C., Pounds, K. A., Boyle, B. J., & Griffiths, R. E. 1991, *Nature*, 353, 315
 Stocke, J. T., Morris, S. L., Gioia, I. M., Maccacaro, T., Schild, R., Wolter, A., Fleming, T. A., & Henry, J. P. 1991, *ApJS*, 76, 813
 Windhorst, R. A., et al. 1992, in preparation
 Woltjer, L., & Setti, G. 1982, in *Astrophysical Cosmology*, ed. H. A. Bruck, G. V. Coyne, S. J., & M. S. Longair (Vatican City: Pontificia Academia Scientiarum), 293